

NASA Technical Memorandum 81419

(NASA-TM-81419) ANALYTICAL AND EXPERIMENTAL  
SPUR GEAR TOOTH TEMPERATURE AS AFFECTED BY  
OPERATING VARIABLES (NASA) 29 P N80-18403  
HC A03/MF A01  
CSCL 13I Unclas  
G3/37 47341

ANALYTICAL AND EXPERIMENTAL  
SPUR GEAR TOOTH TEMPERATURE  
AS AFFECTED BY OPERATING  
VARIABLES

Dennis P. Townsend  
Lewis Research Center  
Cleveland, Ohio

and

Lee S. Akin  
Western Gear Corporation  
Industry, California

Prepared for the  
Third International Power Transmission and Gearing Conference  
sponsored by the American Society of Mechanical Engineers  
San Francisco, California, August 18-22, 1980



ANALYTICAL AND EXPERIMENTAL SPUR GEAR TOOTH TEMPERATURE

AS AFFECTED BY OPERATING VARIABLES

by Dennis P. Townsend\*  
Lewis Research Center  
Cleveland, Ohio

and

Lee S. Akin\*\*  
Western Gear Corporation  
Industry, California

ABSTRACT

A gear tooth temperature analysis was performed using a finite element method combined with a calculated heat input, calculated oil jet impingement depth, and estimated heat transfer coefficients. Experimental measurements of gear tooth average surface temperatures and instantaneous surface temperatures were made with a fast response infrared radiometric microscope. Increased oil jet pressure had a significant effect on both average and peak surface temperatures at both high load and speeds. Increasing the speed at constant load and increasing the load at constant speed causes a significant rise in average and peak surface temperatures of gear teeth. The oil jet pressure required for adequate cooling at high speed and load conditions must be high enough to get full depth penetration of the teeth. Calculated and experimental results were in good agreement with high oil jet penetration but showed poor agreement with low oil jet penetration depth.

---

\*Member ASME.

\*\*Fellow ASME.

## NOMENCLATURE

b	Hertzian contact width, m (in.)
$c_p$	specific heat, J/kg K (Btu/lb °F)
$d_i$	oil jet impingement depth, m (in.)
$F_e$	effective face width, m (in.)
f	friction coefficient
$h_j$	heat transfer coefficient for lubricated flank of gear, W/hr m <sup>2</sup> K (Btu/hr ft <sup>2</sup> °F)
$h_s$	heat transfer coefficient sides of gear, W/hr m <sup>2</sup> K (Btu/hr ft <sup>2</sup> °F)
$h_t$	heat transfer coefficient for unlubricated flank of gear, W/hr m <sup>2</sup> K (Btu/hr ft <sup>2</sup> °F)
j	heat conversion factor
k	IR microscope constant
$L_A$	line of action length, m (in.)
m	module
N	number of teeth
$\Delta N$	radiance
$P_d$	diametral pitch module (in <sup>-1</sup> )
q	heat flux, W/hr (Btu/hr)
$q_t$	total heat generated, W/hr (Btu/hr)
V	rolling velocity, m/sec (ft/sec)
$\Delta V$	IR microscope measured, Volts
$V_g$	gear pitch line velocity, m/sec (ft/sec)
$V_j$	oil jet velocity, m/sec (ft/sec)
$V_s$	sliding velocity, m/sec (ft/sec)
W	normal tooth load, N (lb)

$W_t$	tangential tooth load, N (lb)
$\alpha$	oil jet angle from radial degrees
$\beta$	temperature coefficient of viscosity
$\delta_i$	dimensionless impingement depth, $d_i P_d$ , $m^2$ (in.)
$\epsilon$	emissivity
$\eta$	rotation angle revolutions
$\theta_s$	temperature, K ( $^{\circ}F$ )
$\theta_w$	gear rotation angle from tip of tooth to impingement point, rad
$\kappa$	thermal conductivity, W/m K (Btu/ft $^{\circ}F$ )
$\Lambda$	partition constant
$v_i$	dimensionless oil jet velocity
$\rho$	density, $kg/m^3$ (lb/in $^3$ )
$\rho_{1,2}$	involute radius of curvature, m (in.)
$\phi$	contact angle, rad
$\omega$	angular velocity, rad/sec

### INTRODUCTION

There are several methods of lubricating and cooling gear teeth. These are splash lubrication, drip feed, air/oil mist, and pressurized oil jet flow. The method of successful lubrication usually depends on the operating conditions. For gears operating at moderate to high speed (above 5000 rpm) the pressurized oil jet becomes necessary to provide adequate lubrication and cooling and to prevent scoring of the gear tooth surfaces. Scoring is a result of having a too thin elastohydrodynamic (EHD) oil film. This thin EHD film is usually caused by inadequate cooling rather than insufficient lubricant.

Of the three primary modes of gear tooth failure, scoring is the most common and the most difficult to analyze. A considerable amount of work has

been done over the past four decades to produce quantitative analysis procedures to evaluate the risk of scoring in lubricated gear drives [1,2]. For the first 30 years of this time period most of the concentrated effort had to do with developing a procedure to evaluate the incipient onset of the scoring phenomenon. It has only been in the last decade or so that a concentrated effort has been provided to evaluate the contribution of the gear tooth bulk temperature on the scoring phenomenon and to determine its contribution in bringing about the onset of this failure mode [3,4].

A computer program was developed using a finite element analysis to predict gear tooth temperatures [5,6]. However, this program did not include the effects of oil jet cooling and oil jet impingement depth. It used an average surface heat transfer coefficient for surface temperature calculation based on the best information available at that time.

In order to have a better method for predicting gear tooth temperature, it is necessary to have an analysis that allows for the use of a heat transfer coefficient for oil jet cooling coupled with a coefficient for air/oil mist cooling for that part of the time that each condition exists. Once the analysis can make use of these different coefficients it can be combined with a method that determines the oil jet impingement depth to give a more complete gear temperature analysis program. However, both the oil jet and air/oil mist heat transfer coefficients are unknowns and must be determined experimentally.

The objectives of the work reported herein were to (a) further develop the gear temperature analysis computer program of [5,6] incorporating different heat transfer coefficients for air/oil and oil jet cooling, (b) combine that program with a program developed to determine the impingement depths, and (c) experimentally measure gear tooth temperatures to compare

with those predicted using the improved analysis.

## APPARATUS AND PROCEDURE

### Gear Test Apparatus

Gear tooth temperature measurements were made using the NASA gear test rig (Fig. 1). This test rig uses the four square principle of applying the test gear load so that the input drive needs only to overcome the frictional losses in the system. The rig is described more fully in [7]. The belt driven test rig can be operated at several fixed speeds by changing pulleys. The operating speeds for the test reported herein were 2500, 7500, and 10 000 rpm.

The gear surface temperatures were measured with a fast response infrared radiometric (IR) microscope (Fig. 2) that uses a liquid nitrogen cooled detector. The IR microscope can measure transient temperatures up to 20 000 Hertz. All radiance measurements were made with a 1X lens that has a focal length of approximately 23 cm (9 in.) and a viewing spot size of 0.05 cm (0.020 in.) diameter. The test gear cover, viewing port and lubrication jet as shown in Fig. 3 was used with the IR microscope.

### Test Gears

Dimension of the test gears are shown in Table 1. All gears had a nominal surface finish on the tooth flank of 0.406 micrometer (16  $\mu$ in.) rms and a standard 20° involute profile without tip relief. The test gears were manufactured from consumable electrode vacuum melted (CEVM) AISI 9310. The gears were case carburized and hardened to a Rockwell C hardness of 60 before final grinding of the finished gear.

### Test Lubricant

The test gears were lubricated with a single batch of synthetic paraffinic oil. The physical properties of the oil are summarized in Table 2.

Five percent of an extreme pressure additive, designated Lubrizol 5002 (partial chemical analysis, Table II), was added to the lubricant.

#### Test Procedure

After the test gears were cleaned to remove the presevative, they were assembled on the test rig. The test gears were run in a full face load condition on the 0.635 cm (0.250 in.) face width. The tests were run at four speeds, 2500, 6000, 7500, and 10 000 rpm; three tangential loads of 1895 N/cm (1083 lb/in.), 3736 N/cm (2135 lb/in.), and 5903 N/cm (3373 lb/in.); five oil jet pressures of  $96 \times 10^4$  N/m<sup>2</sup> (140 psi),  $69 \times 10^4$  N/m<sup>2</sup> (100 psi),  $41 \times 10^4$  N/m<sup>2</sup> (60 psi),  $27 \times 10^4$  N/m<sup>2</sup> (40 psi), and  $14 \times 10^4$  N/m<sup>2</sup> (20 psi); and two oil jet diameters of 0.04 cm (0.016 in.), 0.08 cm (0.032 in.). Inlet oil temperature was constant at 308 K (95° F). At each speed the lowest load was first applied with the maximum oil jet pressure. At this load the oil jet pressure was reduced in steps to the lowest pressure before the next load was applied. The oil jet was pointing in a radial direction and hitting the unloaded side of the gear tooth as it came out of the mesh zone. The 0.08 cm (0.032 in.) diameter jet is the size typically used in many applications for the maximum power conditions used herein. The 0.04-cm (0.016-in.) diameter jet was used to determine what cooling conditions could be obtained with considerably less oil flow and good oil jet impingement depth. The temperature was measured by the IR scope at a location approximately 160° away from the mesh zone.

The IR scope operates in two modes. In the DC mode of operation the average surface temperature of the gear tooth was read out on the meter supplied with the IR scope. The scope was calibrated prior to running the tests to determine the emissivity of the gear tooth surface.

In the AC mode of operation a voltage that varies with surface radiance according to the equation

$$\Delta V = K\epsilon \Delta N \quad (1)$$

was measured from two signals on a dual trace cathode ray oscilloscope (CRO). One signal was from the IR scope directly while the second signal was filtered through a variable band pass filter to remove the 20 millivolt high frequency noise. At the lower loads and at the high oil jet pressures the signal to noise ratio was approximately one.

A 1X lens which had a focal length of 23 cm (9 in.) was used with the IR microscope and looked at a 0.05 cm (0.02 in.) diameter spot. The gear tooth surface was viewed by the IR scope as it passed in front of the lens. The tip of the tooth is seen first, the view then goes down the tooth surface until it is interrupted by the next tooth.

#### GEAR TEMPERATURE ANALYSIS

A gear tooth temperature analysis was developed in [5,6] to calculate the gear tooth temperature profile using a finite element analysis. This analysis uses a finite element mesh as shown in Fig. 4 and calculates isotherms on the gear tooth. However, the following are required to be determined or calculated before the program can calculate effective temperatures: (a) the frictional heat input at the gear tooth working surface, (b) the different heat transfer coefficients for the various gear tooth surfaces and cooling methods, and (c) the oil jet penetration onto the gear tooth flank.

The frictional heat input to the gear tooth working surface can be calculated using the following analysis. The instantaneous heat generated per unit area, per unit time due to the sliding of the two gear teeth is given by



$$q = \frac{fW|V_s|}{bJ} = \frac{fW|\omega_1\rho_1 - \omega_2\rho_2|}{bJ} \quad (2)$$

where

$$W = W_t/F_e \cos \phi$$

Since  $W$ ,  $V_s$ , and  $f$  are functions of the mesh point location, the  $q$  will vary through the meshing cycle. The  $f$  varied from approximately 0.02 to 0.07 for the cases evaluated. The heat generated will be divided between the gear and pinion and may not be equal withdrawn by each so that a partitioning function  $\Lambda$  is used. The heat withdrawn by the gear and pinion will then be

$$q_1 = \Lambda q \quad q_2 = (1 - \Lambda)q \quad (3)$$

For the test gears used in this paper  $\Lambda$  is assumed to be 0.5 so that

$$q_1 = q_2 \quad (4)$$

once the instantaneous heat flux to the gear surface is determined, the total time average heat flow per revolution can be calculated by the following equation from [6]

$$q_1 = \frac{b\omega_1\Lambda q}{V_1 2\pi} = \frac{b\omega_2(1 - \Lambda)q}{V_2 2\pi} \quad (5)$$

where  $V_1$  and  $V_2$  are the gear and pinion rolling velocities. Substituting equation (2) into equation (5) gives

$$q_1 = q_2 = \frac{b_1\omega_1\Lambda fW\omega_1}{V_1 2\pi bJ} \left| \rho_1 - \frac{\omega_2}{\omega_1} \rho_2 \right| \quad (6)$$

substituting

$$\Lambda = 0.5, \quad \eta_1 = \frac{\omega_1}{2\pi}, \quad \frac{\omega_2}{\omega_1} = \frac{N_1}{N_2}, \quad \text{and} \quad V_1 = \omega_1\rho_1$$

gives

$$q_1 = q_2 = \frac{fW\eta_1}{2J} \left| 1 - \frac{N_1}{N_2} \frac{\rho_2}{\rho_1} \right| \quad (7)$$

for the time average heat flux. Using this expression, the instantaneous heat flux may be calculated at any position along the line of action by substituting the instantaneous profile radius, giving the heat input to the gear tooth surface at that location. Substituting  $L_A - \rho_1$  for  $\rho_2$  where  $L_A = \rho_1 + \rho_2$  and using instantaneous notation equation (7) becomes

$$q_{i1} = \frac{f_i W \eta_1}{2J} \left| 1 - \frac{N_1}{N_2} \left( \frac{L_A - \rho_{i1}}{\rho_{i1}} \right) \right| \quad (8)$$

The heat transfer coefficients shown in Fig. 5 for the sides, top-land and flanks of the gear teeth are different because of the different cooling regions. Also, the coefficient for the two flanks will be different depending on whether they are cooled by the oil jet hitting the surface or if they are air cooled when no jet cooling is present. The heat transfer coefficient for the sides of the gear teeth  $h_s$  can be estimated by the method of [9] for a rotating disk by

$$h_s = Nu K \sqrt{\frac{\omega}{\nu}} \quad (9)$$

for air  $Nu = 0.5$ . However, the amount of oil mist present will have a considerable effect on this coefficient. The gear tooth flanks not cooled by the oil jet will have a heat transfer coefficient  $h_t$  for air or air/oil mist. Since there is no data available to determine this coefficient, an estimate somewhere between an air-cooled disk and jet cooling will be used until something better is developed experimentally.

The heat transfer coefficient  $h_j$  for the tooth face and the tooth tip that is jet cooled may be calculated from [4,8] using the following

$$h_j = \left(\frac{2L_t}{m}\right)^{1/4} \left(\frac{V_o}{N}\right)^{1/4} \frac{b\omega^{1/2}}{2\pi} q_{tot} \quad (10)$$

where  $q_{tot}$  is a dimensionless factor given in [4,8]. Curve fitting the data from [8] gives

$$q_{tot} = 0.98 - 0.32 \gamma + 0.06 \gamma^2 - 0.004 \gamma^3 \quad (11)$$

where

$$\gamma = \beta \theta_s \quad (12)$$

Using the above method for calculating the oil jet heat transfer coefficient gives results that are much too high. This is because the actual thickness of the oil film conducting heat away from the tooth surface is much thinner than those calculated by the above method. For the results presented in this paper, an oil jet heat transfer coefficient was assumed that would give more realistic results. For future work, a more realistic oil jet heat transfer coefficient will be determined based on experimental results reported in this paper and from future testing.

The oil jet penetration onto the gear tooth flank can be determined by the method of [10,11]. However, a more accurate analysis is being developed by the authors using a new kinematic radial model instead of the vectorial model used in [10]. The new model gives the oil jet impingement depth for radially directed jet as

$$\delta_i = \frac{v_j \theta_\omega (N + 2) \cos \alpha}{4} \quad (13)$$

Using the above equation with a known jet velocity, the angle of rotation is assumed and must be iterated until the angle of rotation and impingement point coincide, since  $\theta_\omega$  is a function of  $\delta_i$  and  $\alpha$ . A more usual case

is when a specified design depth  $\delta_i$  is required and the jet velocity is calculated using a known  $\delta_i$  and  $\theta_\omega$ . Equation (13) is rearranged as

$$v_j = \frac{4\delta_i}{\theta_\omega (N + 2) \cos \alpha} \quad (14)$$

Once the heat generation and the oil jet impingement depth have been calculated, the heat transfer coefficients are either calculated or estimated. Then, the finite element analysis is used to calculate the temperature profile of the gear teeth. The finite element model has 108 nodes with triangular elements. The computer program calculates a steady state temperature at all 108 nodes and prints out these temperatures. The program also plots temperature isobars on the gear tooth profile and lists the temperatures of the isobars.

## RESULTS AND DISCUSSION

### Experimental Results

Transient and average gear tooth surface temperatures were measured using a fast response infrared (IR) radiometric microscope. The gear tooth temperatures were measured at four speeds, three loads, five oil jet pressures, and two oil jet diameters. The test gears were 3.2 module (8 pitch), 8.89 cm (3.5 in.) pitch diameter with a 0.64-cm (0.25-in.) face width.

Figure 6(a) is a typical transient measurement of a gear tooth surface at 7500 rpm, 5903 N/cm (3373 lb/in.) tangential load and  $14 \times 10^4 \text{ N/m}^2$  (20 psi) oil jet pressure with a 0.041-cm (0.016-in.) diameter orifice. The change in surface temperature from the gear tooth tip to a point just below the pitch line was 32 K (58° F). The pitch line where pure rolling occurs can be seen by the slight dip in temperature. The highest temperature is below the pitch line where the combination of high load with some sliding occurs.

Figure 6(b) is the same load, speed and oil jet size condition but with an oil jet pressure of  $97 \times 10^4 \text{ N/m}^2$  (140 psi) which reduces the maximum temperature difference to 12 K ( $22^\circ \text{ F}$ ) with the peak temperature still occurring below the pitch line. The average surface temperature for these conditions was 423 K ( $302^\circ \text{ F}$ ) and 391 K ( $244^\circ \text{ F}$ ) for the  $14 \times 10^4 \text{ N/m}^2$  (20 psi) and  $97 \times 10^4 \text{ N/m}^2$  (140 psi) oil pressure, respectively. Figure 7 is typical of what happens when scoring occurs. Here the peak temperature is at the tip of the gear tooth and has reached a maximum temperature of 508 K ( $455^\circ \text{ F}$ ) or 75 K above the average surface temperature of 433 K ( $320^\circ \text{ F}$ ). Scoring temperatures as high as 603 K ( $626^\circ \text{ F}$ ) were measured during the high-load, high-speed tests with reduced oil jet pressure or orifice size. These temperatures would be somewhat lower than those at the contact point since they were measured 160 degrees away from the contact and after oil jet cooling. The scoring conditions occurred only at the 10 000 rpm test condition with intermediate loads and full or less oil jet impingement depths.

Figure 8(a) is a plot of gear tooth average surface temperature (solid line) with the high and low temperatures included (dotted lines) versus oil jet pressure for three speed, an oil-jet diameter of 0.04 cm (0.016 in.) and a load of 5903 N/cm (3373 lb/in.).

The high load and high speed with the small jet size could not be run except at the highest pressure because of scoring. From these plots, the effect of different speed at constant load and the effect of oil jet pressure on both average surface temperature and temperature variations can be seen. The increased speed causes a higher surface temperature and higher temperature variations. The oil jet pressure also has a greater effect at the higher speed. The maximum oil pressure needed for a speed is also seen

by the leveling of the curve at the lower speeds where increased oil pressure causes very little improvement in cooling.

Figure 8(b) is the same type plot as Fig. 8(a) except the load is 3736 N/cm (2135 lb/in.). The curve for 5000 and 2500 rpm are nearly identical. The effect of oil jet pressure is considerably reduced because of the lower load. Here the maximum change in average surface temperature is 35 K and the maximum surface temperature difference is 45 K at the  $13.8 \times 10^4$  N/m<sup>2</sup> (20 psi) oil jet pressure.

Figure 8(c) is a plot of gear tooth average surface temperature versus oil jet pressure with different loads at a speed of 7500 rpm. This figure shows the effect of load and oil jet pressure on gear tooth temperature at constant speed.

Figure 9 is a plot of load versus gear tooth average surface temperature for the 7500 rpm condition and three oil jet pressures. The effect of load and oil jet pressure on gear tooth surface temperature is clearly seen. Increasing the pressure from  $14 \times 10^4$  N/m<sup>2</sup> (20 psi) to  $97 \times 10^4$  N/m<sup>2</sup> (140 psi) has about the same effect as reducing the load from 6000 to 2000 N/cm.

Figures 10(a) and (b) are plots of average surface temperatures with temperature variations and bulk gear temperature, respectively, versus oil jet pressure for three loads at 10 000 rpm and an oil jet size of 0.08 cm (0.032 in.). With the larger oil jet size the temperatures are reduced considerably from those for the smaller jet size. The bulk temperature of the gear does not increase as much as the average surface temperature. At the lower load and high jet pressure the surface and bulk temperatures are nearly identical.

## Analytical Results

Calculations were made using the analytical program to examine the effects of calculated heat inputs from the experimental test cases and estimated heat transfer coefficients. The differential temperature profiles are shown in Figs. 11 through 14. The differential profiles in these figures are the temperature difference between the inlet cooling oil and the actual gear tooth temperatures.

Matching the analytical predictions with the experimental results is difficult because of different physical conditions existing in the program input and the experiment. The analysis and the tests were planned whereby heat removal was on the working face of the gear tooth. The analysis was completed before the tests were conducted. Initial testing result in oil splashing on the infrared microscope viewing port which prevented meaningful IR temperature measurements. In order to prevent this condition from occurring, the oil jet was directed at the back side of the tooth resulting in cooling of the unloaded side of the gear tooth.

Referring to Fig. 11(a) the conditions were 10 000 rpm with a tangential tooth load of 5903 N/cm (3373 lb/in.) and an impingement depth of zero. This means that the gear had impingement on the topline only. The lowest level of temperature difference in the gear tooth is 35 K (63° F) at the tip of the tooth. The hot spot is just below the pitch line and is 122 K (200° F) above the oil jet temperature. This gives an average surface temperature above oil jet temperature of approximately 79 K (142° F). The lowest temperature is much cooler than that of similar experimental conditions. However, the hot spot is only a little cooler than the experimental data which indicates better oil cooling is assumed for the analysis than that obtained experimentally.

Figure 11(b) is a gear tooth temperature profile for the same conditions as Fig. 11(a) except that the oil jet impingement is 87.5 percent of the tooth depth. Here the minimum temperature difference is at the tooth tip of 9 K ( $16^{\circ}$  F) and the highest temperature difference just below the pitch line is 31 K ( $56^{\circ}$  F). This is somewhat cooler than a similar experimental case as shown in Fig. 10 where the temperature difference for the maximum temperature is 63 K ( $113^{\circ}$  F) and the minimum is 49 K ( $88^{\circ}$  F). The difference between the maximum and minimum temperature is 22 K ( $40^{\circ}$  F) for the analytical and 14 K ( $25^{\circ}$  F) for the experimental. Here the analytical and experimental are not extremely different indicating a close choice for the analytical oil jet cooling.

Figure 12(a) is the analytical gear tooth temperature for operating conditions of 7500 rpm, a tooth load of 5903 N/cm (3373 lb/in.) , and an impingement depth of zero or topline cooling only. Here the lowest temperature difference is also at the tooth tip and is 27 K ( $49^{\circ}$  F) and the hot spot is below the pitch point and is 96 K ( $173^{\circ}$  F). A similar test condition is shown in Fig. 8(a) when a small jet diameter was used and the minimum and maximum temperature differences were 101 K ( $182^{\circ}$  F) and 133 K ( $239^{\circ}$  F), respectively. Here again the minimum temperature for the analytical case is much cooler while the maximum temperature is somewhat closer to that for the experimental case.

Figure 12(b) is the tooth temperature profile for the same conditions as Fig. 12(a) except that the oil jet impingement depth is 87.5 percent of the tooth depth. Here the minimum temperature difference between oil jet and gear is 7 K ( $13^{\circ}$  F) at the tip and the maximum temperature difference below the pitch point is 24 K ( $43^{\circ}$  F). The similar test condition is shown in Fig. 8(a) where the minimum and maximum temperatures were 51 K ( $92^{\circ}$  F)



and 68 K (122° F) above the oil jet temperature, respectively. As a result, at the lower speed the analytical oil jet cooling is more than that obtained experimentally.

Figure 13(a) is the analytical results for an operating condition of 7500 rpm, a tangential tooth load of 1895 N/cm (1083 lb/in.) and an impingement depth of zero. The minimum temperature difference between the oil jet and tooth temperature is at the tooth tip and is 16 K (29° F) while the maximum temperature of 50 K (90° F) is below the pitch point. The similar test conditions shown in Fig. 8(c) give a minimum temperature difference of 67 K (121° F) and a maximum temperature difference of 120 K (216° F) between oil jet and gear tooth temperatures. The temperature difference between the analytical and experimental case is still considerably different at this lower load and speed.

Figure 13(b) is the same condition as Fig. 13(a) except for the oil jet impingement depth of 87.5 percent of the tooth depth. The minimum and maximum oil jet to gear tooth temperatures of 4 K (7° F) and 12 K (22° F) are considerably cooler than the experimental minimum and maximum oil jet to gear tooth temperature of 38 K (68° F) and 47 K (85° F), respectively, shown in Fig. 8(c).

Considering the differences in the analytical and experimental methods of cooling the gear teeth and the estimation used to obtain heat transfer coefficients, the difference between the analytical and experimental results are not unreasonable. Additional work with experimental and analytical gear tooth cooling should resolve these differences without much difficulty.

## SUMMARY OF RESULTS

A gear tooth temperature analysis was performed using a finite element method combined with a calculated heat input, a calculated oil jet impingement depth and estimated heat transfer coefficients for the different parts of the gear tooth that are oil cooled and air cooled. Experimental measurements of gear tooth average surface temperature and gear tooth instantaneous surface temperature were made with a fast response, infrared radiometric microscope. The following results were obtained.

1. Increased oil pressure has a significant effect on both average surface temperature and peak surface temperature at loads above 1895 N/cm (1083 lb/in.) and speeds of 10 000 and 7500 rpm.

2. Increased speed from 5000 to 10 000 rpm at constant load and increased load at constant speed causes a significant rise in the average surface temperature and the instantaneous peak surface temperatures on the gear teeth.

3. The oil jet pressure required to provide the best cooling for gears is the pressure required to obtain full gear tooth penetration depth.

4. Calculated results for gear tooth temperatures were reasonably close to experimental results for high oil jet penetration depths but was significantly different for low oil jet penetration depths.

## REFERENCES

1. Blok, H., "Lubrication as a Gear Design Factor," The Institution of Mechanical Engineers, Proceedings of the International Conference on Gearing, London, Sept. 23rd-25th, 1958.
2. Kelley, B. W. and Lemanski, A. J., "Lubrication of Involute Gearing," Institution of Mechanical Engineers, Proceedings (Fundamentals & Application to Design), Vol. 182, Pt. 3A, 1967-1968, pp. 173-184.

3. Akin, L. S., "An Interdisciplinary Lubrication Theory for Gears (With Particular Emphasis on the Scuffing Mode of Failure)," ASME Journal of Engineering for Industry, Vol. 95, No. 4, Nov. 1973, pp. 1178-1195.
4. DeWinter, A. and Blok, H., "Fling-Off Cooling of Gear Teeth," ASME Journal of Engineering for Industry, Vol. 96, No. 1, Feb. 1974, pp. 60-70.
5. Wang, K. L. and Cheng, H. S., "A Numerical Solution to the Dynamic Load, Film Thickness, and Surface Temperatures in Spur Gears, Part II - Results," ASME International Power Transmission and Gear Conference, Chicago, IL, Sep. 28-30, 1977.
6. Patir, N. and Cheng, H. S., "Prediction of Bulk Temperature in Spur Gears Based on Finite Element Temperature Analysis," ASLE Preprint No. 77-LC-3B-2, Oct. 1977.
7. Townsend, D. P., Bamberger, E. N., and Zaretsky, E. V., "A Life Study of Ausforged, Standard Forged, and Standard Machined AISI M-50 Spur Gears," ASME Journal of Lubrication Technology, Vol. 98, No. 3, July 1976, pp. 418-425.
8. Van Heijningen, G. J. J. and Blok, H., "Continuous as Against Intermittent Fling-Off Cooling of Gear Teeth," ASME Journal of Lubrication Technology, Vol. 96, No. 4, Oct. 1974, pp. 529-538.
9. Patir, N., "Estimate of the Bulk Temperature in Spur Gears Based on Finite Element Temperature Analysis," M.S. Thesis, Northwestern University, 1976.
10. Akin, L. S., Mross, J. J., and Townsend, D. P., "Study of Lubricant Jet Flow Phenomena in Spur Gears," ASME Journal of Lubrication Technology, Vol. 97, No. 2, Apr. 1975, pp. 283-288.
11. Townsend, D. P. and Akin, L. S., "Study of Lubricant Jet Flow Phenomena in Spur Gears -- Out of Mesh Condition," ASME Journal of Mechanical Design, Vol. 100, No. 1, Jan. 1978, pp. 61-68.

TABLE 1. - SPUR GEAR DATA

[Gear tolerance per ASMA class 12.]

Number of teeth . . . . .	28
Diametral pitch . . . . .	8
Circular pitch, cm (in.) . . . . .	0.9975 (0.3927)
Whole depth, cm (in.) . . . . .	0.762 (0.300)
Addendum, cm (in.) . . . . .	0.318 (0.125)
Chordal tooth thickness reference, cm (in.) . . . . .	0.485 (0.191)
Pressure angle, deg . . . . .	20
Pitch diameter, cm (in.) . . . . .	8.890 (3.500)
Outside diameter, cm (in.) . . . . .	9.525 (3.750)
Root fillet, cm (in.) . . . . .	0.102 to 0.152 (0.04 to 0.06)
Measurement over pins, cm (in.) . . . . .	9.603 to 9.630 (3.7807 to 3.7915)
Pin diameter, cm (in.) . . . . .	0.549 (0.216)
Backlash reference, cm (in.) . . . . .	0.0254 (0.010)
Tip relief, cm (in.) . . . . .	0.00

TABLE 2. - LUBRICANT PROPERTIES

Property	Synthetic paraffinic oil plus additives <sup>a</sup>
Kinematic viscosity, cm <sup>2</sup> /sec (cs) at:	
244 K (-20° F)	2500×10 <sup>-2</sup> (2500)
311 K (100° F)	31.6×10 <sup>-2</sup> (31.6)
372 K (210° F)	5.7×10 <sup>-2</sup> (5.7)
477 K (400° F)	2.0×10 <sup>-2</sup> (2.0)
Flash point, K (°F)	508 (455)
Fire point, K (°F)	533 (500)
Pour point, K (°F)	219 (-65)
Specific gravity	0.8285
Vapor pressure at 311 K (100° F), mm Hg (or torr)	0.1
Specific heat at 311 K (100° F), J/(kg)(K) (Btu/(lb)(°F)) . . .	676 (0.523)

<sup>a</sup>Additive, Lubrizol 5002 (5 percent volume): phosphorus, 0.03 percent volume; sulfur, 0.93 percent volume.

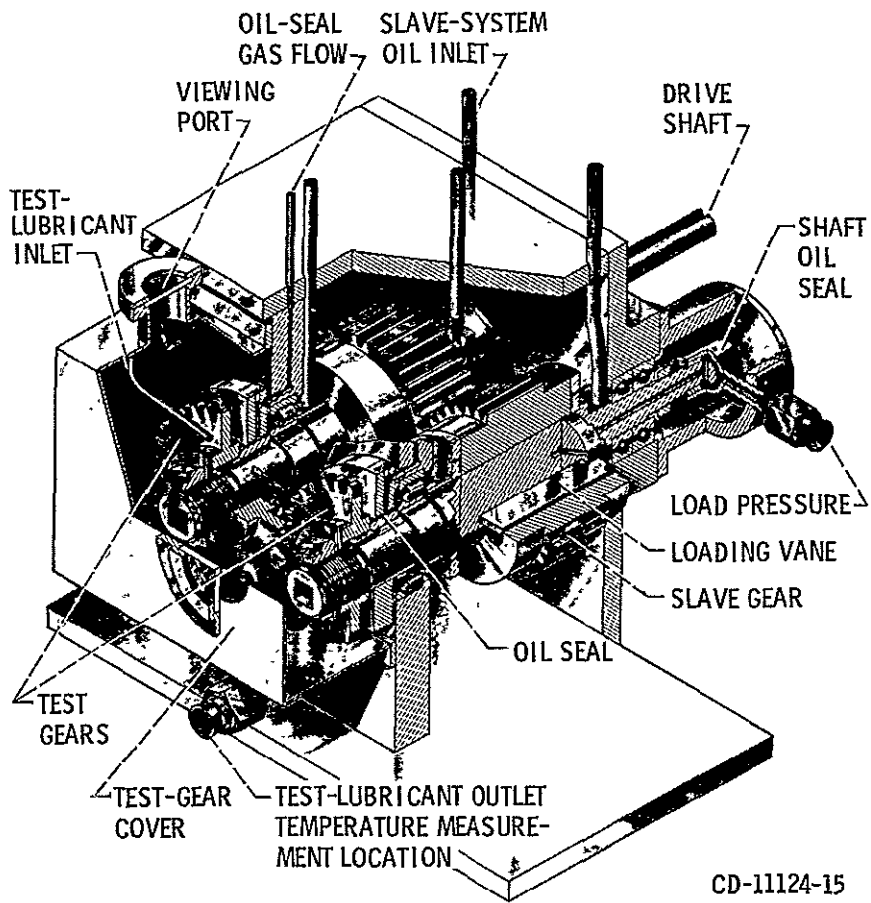


Figure 1. - NASA Lewis Research Center's gear fatigue test apparatus.

ORIGINAL PAGE IS  
 OF POOR QUALITY

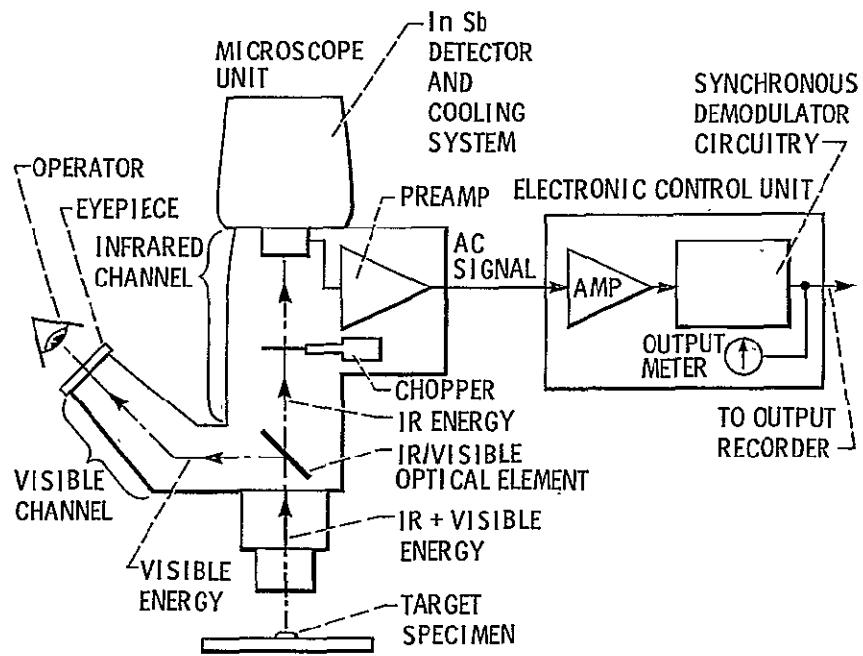


Figure 2. - Simplified functional diagram, infrared radiometric microscope.

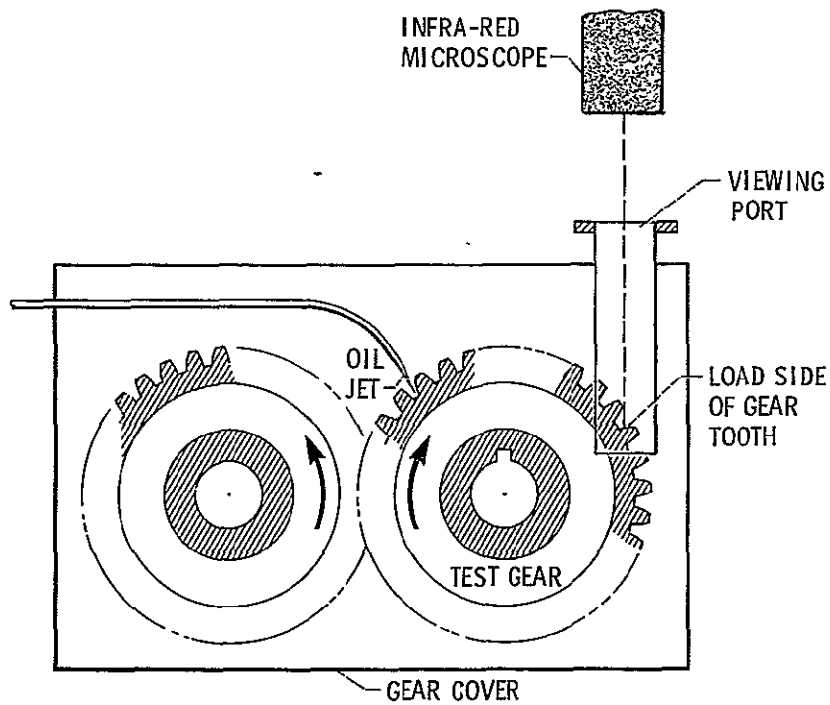


Figure 3. - Test setup for measuring dynamic gear tooth surface temperature.

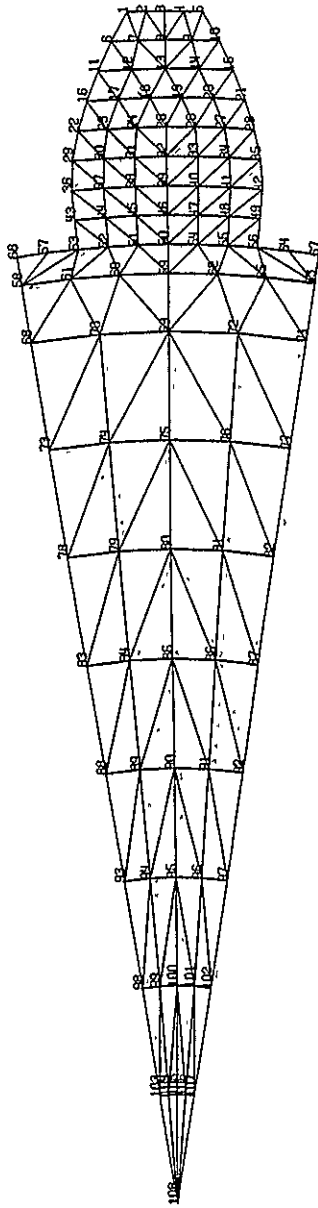
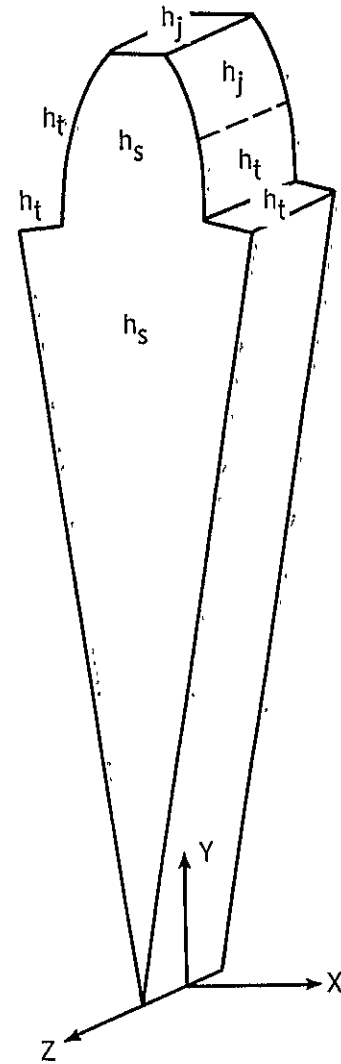
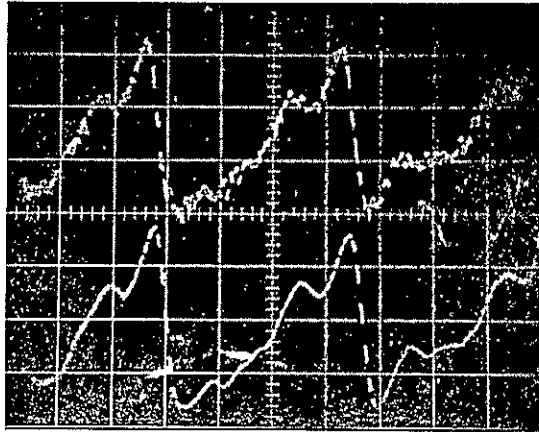


Figure 4. - Finite element mesh.

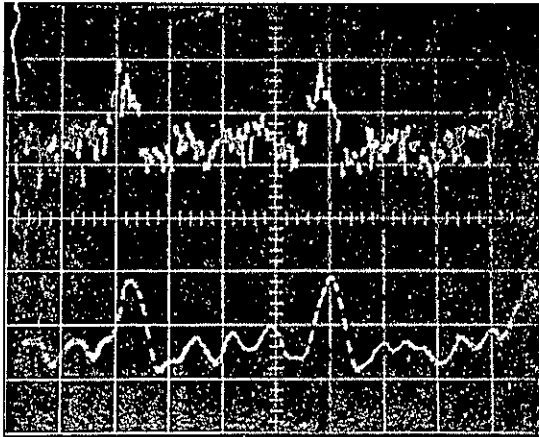


$h_s, h_j, h_t$  = DEFINITION OF  
HEAT TRANSFER ZONES

Figure 5. - Geometry of problem.



(a)  $14 \times 10^4 \text{ N/m}^2$  (20 psi), 0.05 V/div.



(b)  $69 \times 10^4 \text{ N/m}^2$  (100 psi), 0.02 V/div.

Figure 6. - I. R. microscope measurements of gear tooth surface temperature, speed; 7500 rpm load 5903 N/cm (3373 lb/in.) inlet oil temperature 308 K (95<sup>o</sup> F) oil jet diameter 0.04 cm (0.016 in. ).

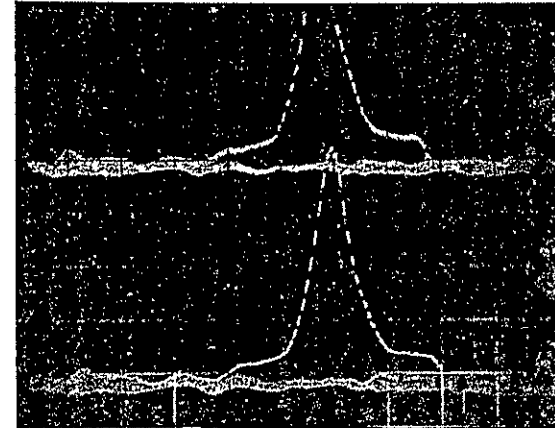


Figure 7. - I. R. microscope measurements of gear teeth scoring temperature 0.5 V/div speed 10 000 rpm load 5903 N/cm (3373 lb/in.) inlet oil temperature 308 K (95<sup>o</sup> F) oil jet diameter 0.04 cm (0.016 in. ).



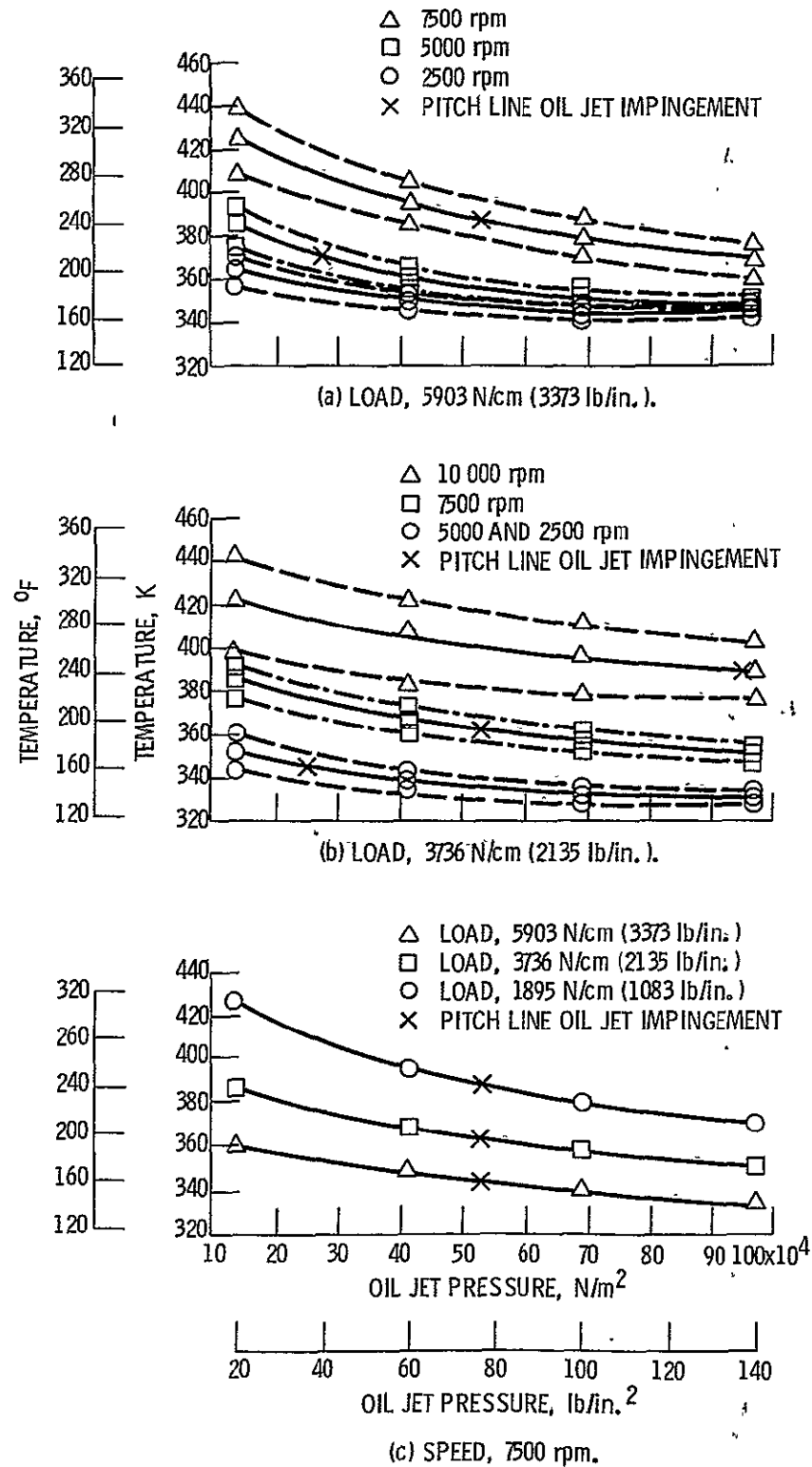


Figure 8. - I. R. microscope measurements of gear surface temperature versus oil jet pressure, inlet oil temperature 308 K (95° F), oil jet diameter 0.04 cm (0.016 in.).

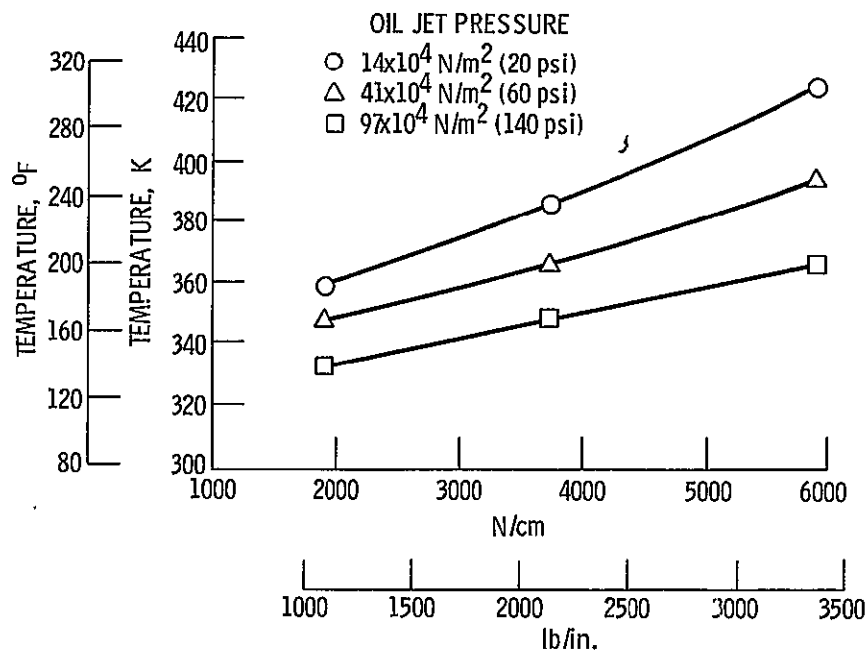


Figure 9. - I. R. microscope measurement of gear average surface temperature versus load for three oil jet pressures, speed 7500 rpm, oil jet diameter 0.04 cm (0.016 in.) inlet oil temperature 308 K (95° F).

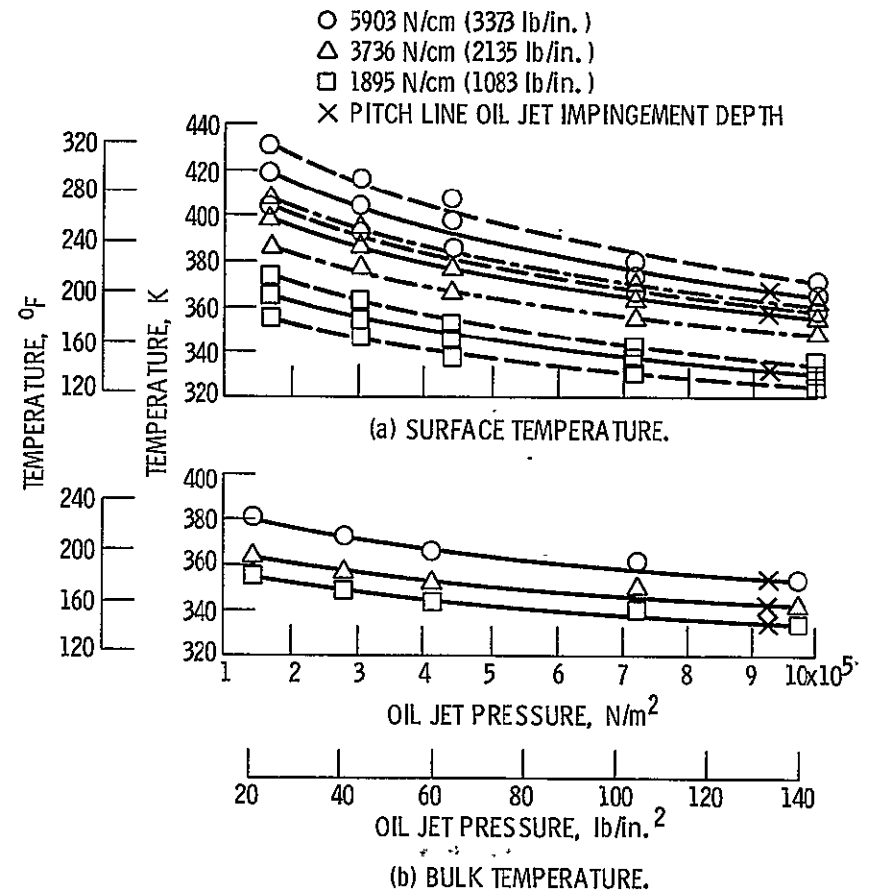
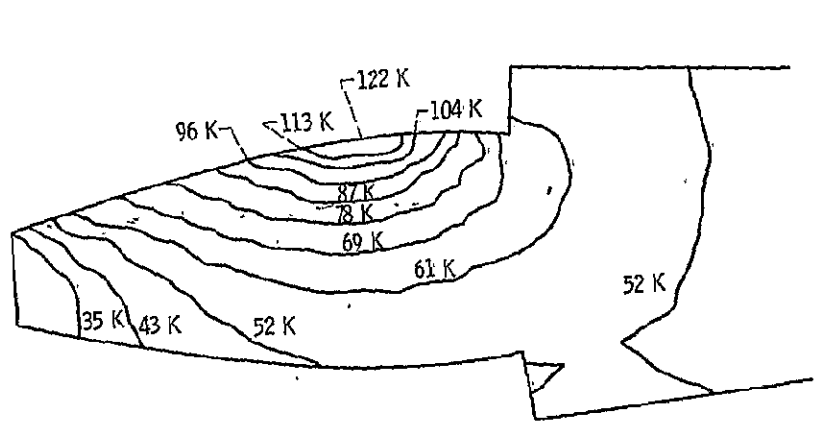
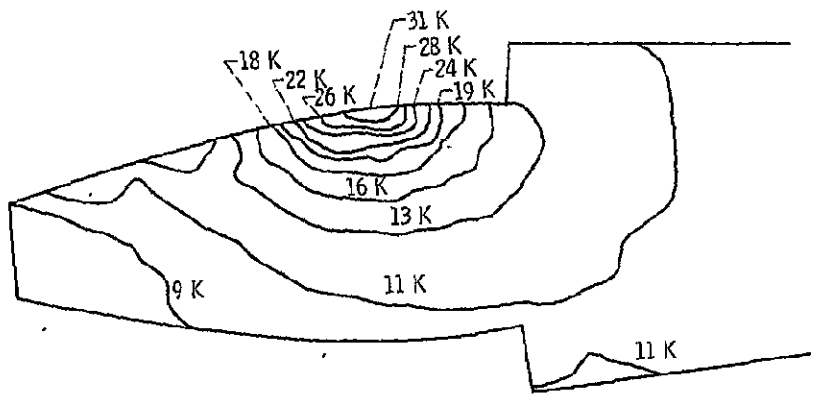


Figure 10. - I. R. microscope and thermocouple measurement of gear temperature versus oil jet pressure for three loads, speed 10 000 rpm, oil jet diameter 0.08 cm (0.032 in.). Inlet oil 308 K (95° F).

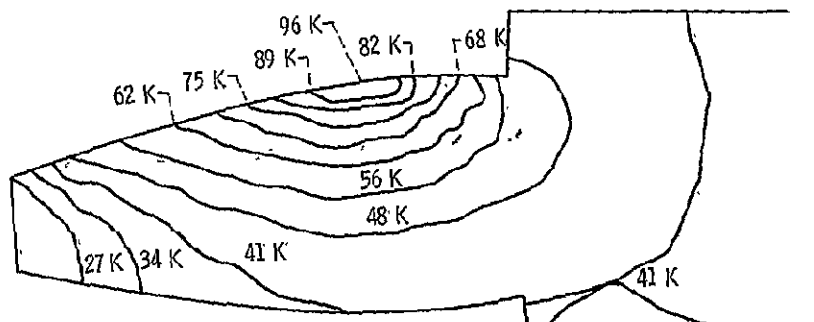


(a) ZERO IMPINGEMENT DEPTH.

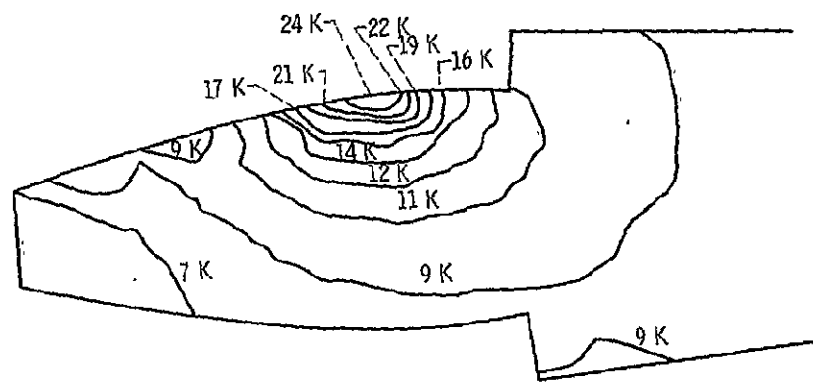


(b) 87.5 percent IMPINGEMENT DEPTH.

Figure 11. - Calculated gear tooth temperatures speed 10 000 rpm, load 5903 N/cm (3373 lb/in. ).

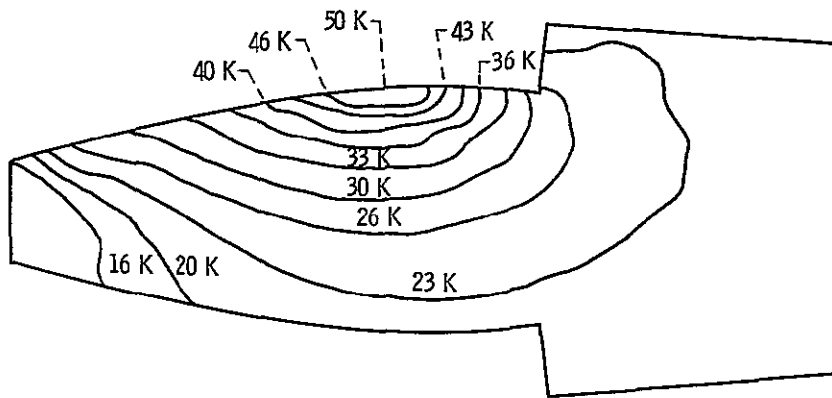


(a) ZERO IMPINGEMENT DEPTH.

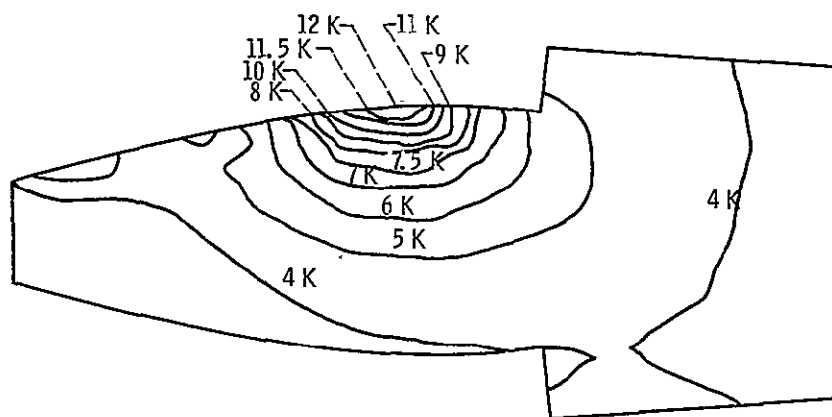


(b) 87.5 percent IMPINGEMENT DEPTH.

Figure 12. - Calculated gear tooth temperatures speed 7500 rpm, load 5903 N/cm (3373 lb/in. ).



(a) ZERO IMPINGEMENT DEPTH.



(b) 87.5 percent IMPINGEMENT DEPTH.

Figure 13. - Calculated gear tooth temperatures, speed 7500 rpm, load 1895 N/cm (1083 lb/in.).

1. Report No. NASA TM-81419	2. Government Accession No.	3. Recipient's Catalog No.	
4. Title and Subtitle ANALYTICAL AND EXPERIMENTAL SPUR GEAR TOOTH TEMPERATURE AS AFFECTED BY OPERATING VARIABLES		5. Report Date	
		6. Performing Organization Code	
7. Author(s) Dennis P. Townsend and Lee S. Akin		8. Performing Organization Report No. E-342	
		10. Work Unit No.	
9. Performing Organization Name and Address National Aeronautics and Space Administration Lewis Research Center Cleveland, Ohio 44135		11. Contract or Grant No.	
		13. Type of Report and Period Covered Technical Memorandum	
12. Sponsoring Agency Name and Address National Aeronautics and Space Administration Washington, D. C. 20546		14. Sponsoring Agency Code	
		15. Supplementary Notes Dennis P. Townsend, Lewis Research Center, Cleveland, Ohio and Lee S. Akin, Western Gear Corporation, Industry, California.	
16. Abstract A gear tooth temperature analysis was performed using a finite element method combined with a calculated heat input, calculated oil jet impingement depth, and estimated heat transfer coefficients. Experimental measurements of gear tooth average surface temperatures and instantaneous surface temperatures were made with a fast response infrared radiometric microscope. Increased oil jet pressure had a significant effect on both average and peak surface temperatures at both high load and speeds. Increasing the speed at constant load and increasing the load at constant speed causes a significant rise in average and peak surface temperatures of gear teeth. The oil jet pressure required for adequate cooling at high speed and load conditions must be high enough to get full depth penetration of the teeth. Calculated and experimental results were in good agreement with high oil jet penetration but showed poor agreement with low oil jet penetration depth.			
17. Key Words (Suggested by Author(s)) Gear lubrication      Infrared microscopy Gear temperature      Oil jet penetration Heat transfer          Oil jet cooling		18. Distribution Statement Unclassified - unlimited STAR Category 37	
19. Security Classif. (of this report) Unclassified	20. Security Classif. (of this page) Unclassified	21. No. of Pages	22. Price

National Aeronautics and  
Space Administration

Washington, D.C.  
20546

Official Business  
Penalty for Private Use, \$300

SPECIAL FOURTH CLASS MAIL  
BOOK

Postage and Fees Paid  
National Aeronautics and  
Space Administration  
NASA-451



**NASA**

POSTMASTER: If Undeliverable (Section 158  
Postal Manual) Do Not Return

---